

# Simple and Low-Cost Electrochemical Sensor Based on Nickel Nanoparticles for the Determination of Cabergoline<sup>1</sup>

Shahla Fathi\*, Shahab Gholitabar Omrani, and Saeed Zamani

Chemistry Department, Islamic Azad University, Ayatollah Amoli Branch Amol, Iran, Zip Code 46178-678

\*e-mail: fathi\_shahla@yahoo.com

Received January 22, 2015; in final form, June 21, 2015

**Abstract**—Cabergoline (CAB) is an ergot alkaloid derivative with dopamine agonist activity. In this work for the first time the electrocatalytic oxidation of CAB was carried out with nickel nanoparticles-modified carbon paste electrode using cyclic voltammetry, chronoamperometry, chronocoulometry and amperometry methods. At first, nickel nanoparticles were synthesized by non-aqueous polyol method and these nanoparticles were mixed with graphite powder to form modified carbon paste electrode. The resulting modified electrode was characterized by scanning electron microscope images. In the presence of 0.1 M NaOH a good redox behavior of the Ni(III)/Ni(II) couple at the surface of the electrode can be observed. CAB was successfully oxidized at the surface of the modified electrode. The electrocatalytic oxidation peak current of this drug was linearly dependent on its concentration. The proposed sensor exhibited a high sensitivity and was successfully applied for the determination of CAB in real samples.

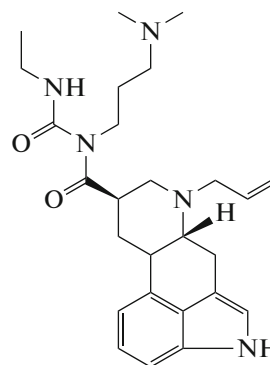
**Keywords:** electrocatalytic oxidation, nickel nanoparticles, non-aqueous polyol method, cabergoline

**DOI:** 10.1134/S1061934816030126

Cabergoline 1-[(6-allylergoline-8 $\beta$ -yl)-carbonyl]-1-[3-(dimethylamino)propyl]-3-ethyl urea (Scheme) is a dopamine agonist licensed for the treatment of Parkinson's disease as adjunctive treatment with levodopa plus a dopa-decarboxylase inhibitor in patients effected by on-off mobility problems [1]. Till now, the commonly employed techniques for the determination of this drug in bulk form, pharmaceutical formulations and biological fluids are based on HPLC [2], LC-MS [3], spectroscopy [4] and microbiological assays [5–9]. The problems encountered using such methods are the need for time-consuming extraction procedures and expensive instrumentation, so the use of a simpler, faster, cheaper and also sensitive electrochemical technique can be an interesting alternative. Electrochemistry has many advantages, making it an appealing choice for pharmaceutical analysis [10, 11]. Electrochemistry has always provided analytical techniques characterized by instrumental simplicity, moderate cost, and portability.

Carbon paste electrode (CPE) has been widely used in determination of drugs, biomolecules and other organic species because of its easy preparation and wide potential window of  $-1.4$  to  $+1.3$  V (versus saturated calomel electrode) [12]. The usefulness of modified carbon paste electrodes in the electroanalytical chemistry has been widely demonstrated, and

their development for analytical applications is still of great interest [13]. Nowadays, it is important to develop new materials such as graphene, nanoparticles, and carbon nanotubes capable to improve the analytical properties of the electrode surface [14, 15]. Among them, nanosized metal particle-modified electrodes have emerged as a promising alternative for the determination of organic and inorganic compounds [16, 17].



**Scheme.** Chemical structure of cabergoline.

Metal nanoparticles have some distinct advantages such as high mass transport rate, low influence of the solution resistance, low detection limits and better signal-to-noise ratio compared to the conventional macroelectrodes [18–20]. They also have a wide range of technological applications including catalysis, optics,

<sup>1</sup> The article is published in the original.

microelectronics, and chemical/biological sensors. Metals in the nanometer range provide three important functions for electroanalysis: roughening of the conductive sensing interface, catalytic properties and conductivity properties [21]. Electrochemical studies have revealed that nickel nanoparticles enhance electrode conductivity and surface area, facilitate the electron transfer, increase the effective electroactive surface area and improve the detection limit of the analytes [22–24]. These properties make nickel nanoparticles a candidate for sensor applications. Previously we reported electrocatalytic oxidation and determination of folic acid [25] and antibiotic drugs [26–28] on nickel/polymeric modified carbon paste electrodes.

In this work, we used the above-mentioned advantageous properties of the nickel nanoparticles-modified carbon paste electrode (Ni-NP/MCPE) for the electrocatalytic oxidation of cabergoline as a dopaminergic drug. A brief glance at the literature indicates that electrocatalytic oxidation of cabergoline has not been reported with nickel catalyst. In this context, nickel nanoparticles were synthesized and mixed with graphite powder to construct the Ni-NP/MCPE. Efficiency of this electrode as a sensor for the electrocatalytic oxidation and determination of cabergoline in alkaline media was investigated.

## EXPERIMENTAL

**Reagents and materials.** All chemicals used in this experiment were of analytical grade and used as received. The solvent used in this work was twice distilled water. Graphite powder (particle diameter: 0.10 mm) was used as the working electrode substrate and also high purity paraffin (density 0.88 g/cm<sup>3</sup>) was used as the pasting liquid for the carbon paste electrode from Fluka. Nickel chloride hexahydrate, 80 wt % hydrazine hydrate (N<sub>2</sub>H<sub>4</sub> · H<sub>2</sub>O), ethylene glycol (EG) that was employed as a surfactant and sodium hydroxide were obtained from Merck.

**Synthesis of nickel nanoparticles.** Nickel nanoparticles were synthesized by a known procedure [29]. In this so-called polyol process which has been extensively exploited by many research groups to synthesize metal particles, EG acts as solvent. In a typical experiment, 60 mL of 15 mM NiCl<sub>2</sub>, 30 mL of 0.15 M N<sub>2</sub>H<sub>4</sub> and an appropriate amount of 1 M NaOH were mixed in a three-neck flask equipped with a stirring bar, a thermometer, a dropping funnel and a condenser. All the reactants were diluted and dissolved in EG. At first, hydrazine was heated to boiling point of the mixture, which was about 184°C. A mixture of Ni<sup>2+</sup> and the appropriate amount of NaOH was added quickly into the heated hydrazine as it reached the boiling point. The temperature was maintained constant at the boiling point of mixture using oil-bath. The temperature was monitored using a thermometer. Initially

the green solution turned into black, indicating the formation of nickel metal. The mixture was heated for 30 min under vigorous stirring. After the reaction was completed, the colloid was cooled to room temperature and the particles were precipitated from the solution by adding ethanol.

**Preparation of working electrode.** A mixture of graphite powder and paraffin was blended by hand mixing with a mortar and pestle for preparation of carbon paste. The resulting paste was then inserted in the bottom of a glass tube (internal radius 2 mm). The electrical connection was implemented by a copper wire lead fitted into the glass tube. A fresh electrode surface was generated rapidly by extruding a small plug of the paste with a stainless steel rod and smoothing the resulting surface on white paper until a smooth shiny surface was observed. A modified paste was prepared in a similar fashion, except that the graphite powder was mixed with 1% (w/w) of nickel nanoparticles.

**Instrumentation.** The electrochemical experiments were carried out using a potentiostat/galvanostat (Sama 500-C Electrochemical Analysis System, Sama, Iran). The three-electrode system consists of the modified carbon paste electrode as working electrode, Ag|AgCl|KCl (3 M) as a reference electrode and a Pt wire as a counter electrode.

**Preparation of a real sample.** In order to analyze the Caberlin® tablets, the average mass of three tablets was calculated. The tablets were finely powdered and homogenized in a mortar. An appropriate accurately weighed amount of the homogenized powder was transferred into a 100 mL calibrated flask containing 50 mL of 0.1 M NaOH solution. The contents of flask were sonicated for 10 min; the undissolved excipients were removed by filtering and the solution was diluted to volume with the same supporting electrolyte. Appropriate solutions were prepared by taking suitable aliquots of the clear filtrate and diluting them with 0.1 M NaOH.

## RESULTS AND DISCUSSION

**Scanning electron microscopy (SEM).** Figure 1a shows the SEM image of nickel nanoparticles, indicating that these particles were well formed with an average size of 50 nm. Figures 1b, 1c show typical SEM images of the unmodified and modified carbon paste electrodes, respectively. It can be seen from the micrograph that the nickel nanoparticles with an average diameter 50 nm were randomly distributed over the surface of carbon paste electrode.

**Electrochemical behavior of the Ni-NP/MCPE.** The polarization behavior of Ni-NP/MCPE was examined in 0.1 M NaOH by using cyclic voltammetry. This technique allows the oxide film formation in parallel to inspecting the electrochemical reactivity of the surface [30]. Voltammograms were recorded by

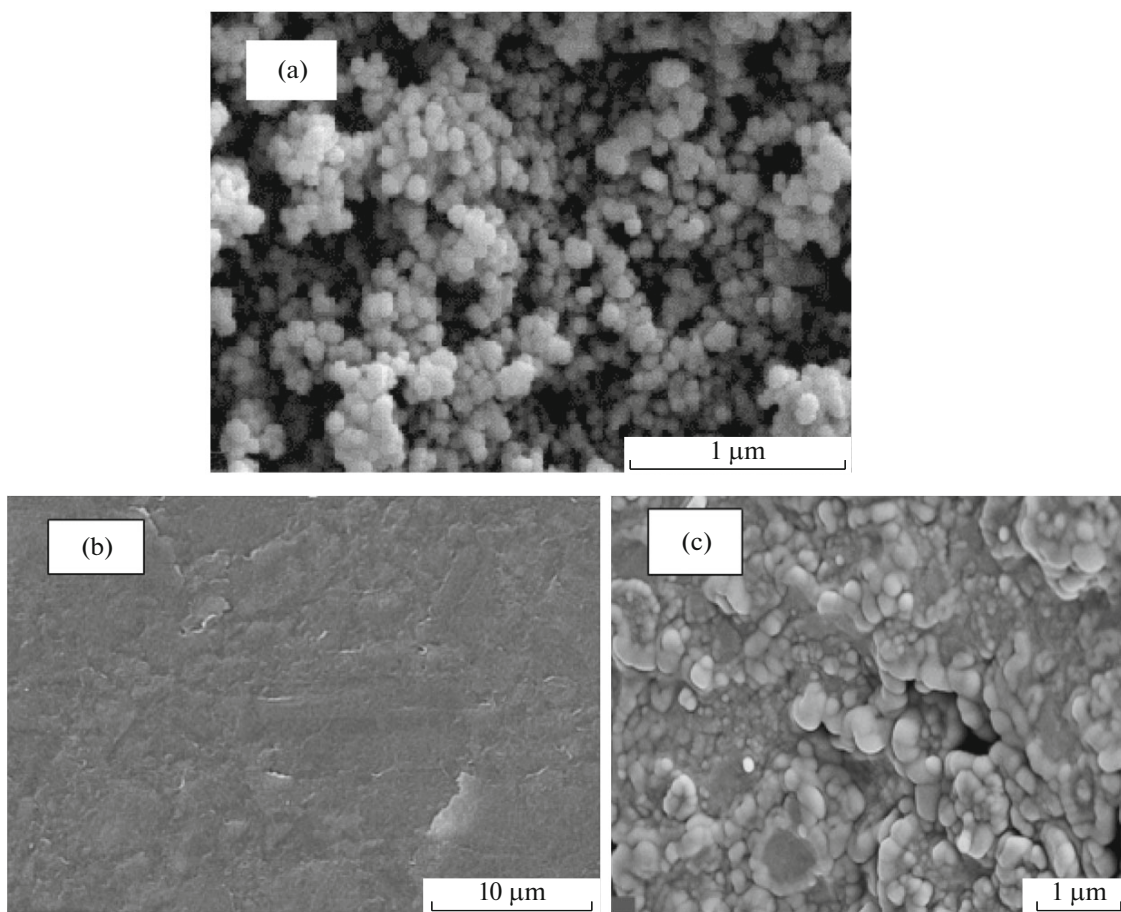


Fig. 1. SEM image of Ni nanoparticles (a), surface of bare CPE (b) and Ni-NP/MCPE (c).

cycling the potential between 0.1 and 0.7 V at 100 mV/s until a stable voltammogram was obtained. Figure 2 shows the electrochemical response of the CPE and Ni-NP/MCPE after polarization in 0.1 M NaOH solution. From Fig. 2 it can be seen that whereas neither oxidation nor reduction took place on the CPE, a well developed redox wave was observed on the Ni-NP/MCPE when the potential was swept and cycled between 0.1 and 0.7 V, which was related to the oxidation of Ni(OH)<sub>2</sub> to NiOOH with a peak potential of 0.46 V and reduction of NiOOH to Ni(OH)<sub>2</sub> with a peak potential of 0.33 V:



An approximate estimate of the amount of incorporated Ni(II) on Ni-NP/MCPE (surface coverage of the electrode) can be evaluated using equation  $\Gamma^* = Q/nFA$ , where  $Q$  is the electric charge obtained by integrating anodic peak obtained at 10 mV/s (Fig. 2, curve 2), with the background correction;  $n$ ,  $F$  and  $A$  represent the number of electrons transferred in redox reaction, Faraday constant and geometric electrode area, respectively. The internal radius of glass

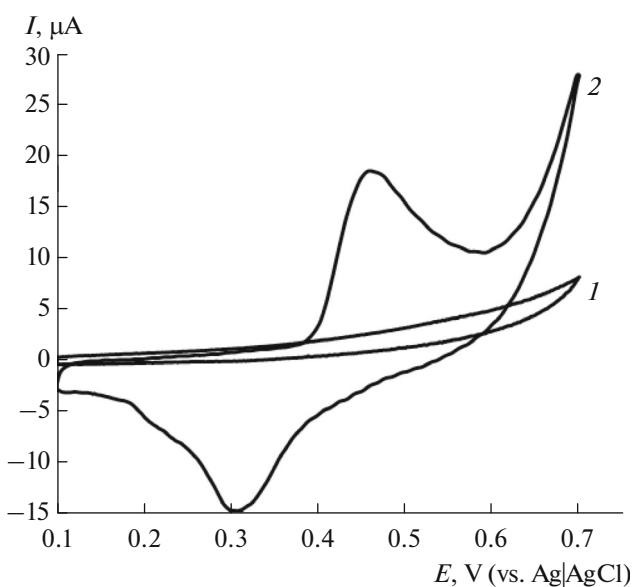
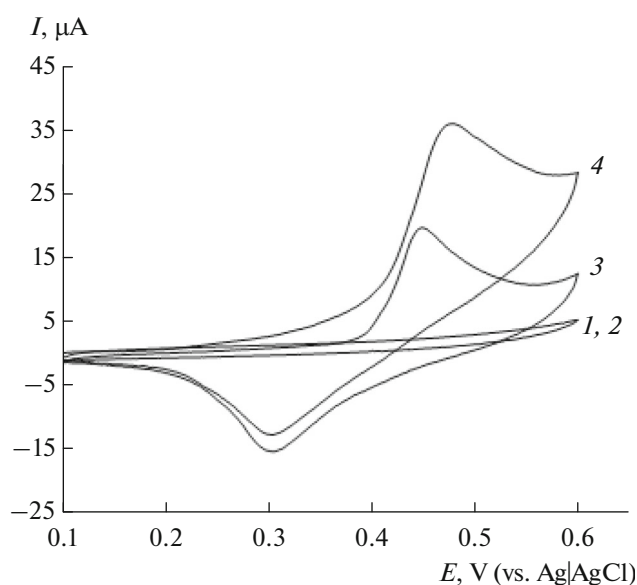


Fig. 2. Electrochemical responses of CPE (1) and Ni-NP/MCPE (2) in 0.1 M NaOH solution, scan rate 10 mV/s.

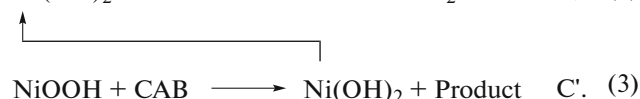


**Fig. 3.** Electrochemical responses of CPE to 0 (1), 0.4 (2) mM cabergoline and Ni-NP/MCPE to 0 (3) and 0.4 (4) mM cabergoline in 0.1 M NaOH solution, scan rate 10 mV/s.

tube  $A = \pi r^2$  was equal to  $0.126 \text{ cm}^2$ . The value of  $\Gamma^*$  for Ni-NP/MCPE was  $3.8 \times 10^{-6} \text{ mol/cm}^2$ .

**Electrocatalytic oxidations of cabergoline on the surface of Ni-NP/MCPE. Cyclic voltammetry studies.** The oxidation of cabergoline was first studied at a CPE (without the integration of nickel nanoparticles)

by cyclic voltammetric experiments in 0.1 M NaOH solution. Typical results obtained for a potential range from 0.1 to 0.6 V vs. Ag|AgCl|KCl (3 M) at potential scan rate of 10 mV/s is shown in Fig. 3. Response of CPE in the absence of CAB is shown in Fig. 3, curve 1; the addition of 0.4 mM CAB to the alkaline solution causes no effect on the electrochemical response of the CPE (Fig. 3, curve 2). The electrochemical response of the Ni-NP/MCPE in 0.1 M NaOH solution exhibits well defined anodic and cathodic peaks (Fig. 3, curve 3) related to the Ni(II)/Ni(III) redox couple. As it is seen in Fig. 3, curve 4, after adding 0.4 mM CAB there is an increase in the anodic peak current and a decrease in the cathodic peak current. This behavior is typical of that expected for the mediated oxidation (EC' mechanism) as follows [31, 32]:



Thus modifier layer of Ni(OH)<sub>2</sub> at the electrode surface acts as a catalyst for the oxidation of CAB in the NaOH solution. Cyclic voltammograms of the Ni-NP/MCPE in the presence of 0.4 mM CAB at various scan rates are recorded in Fig. 4a. With increasing scan rate, the peak potential for the catalytic oxidation of CAB shift to increasingly positive potentials, suggesting a kinetic limitation in the reaction between the redox sites of the Ni-NP/MCPE and CAB. Also, as it can be seen at higher potential scan rates, the cathodic peak current relating to Ni(III) reduction to Ni(II)

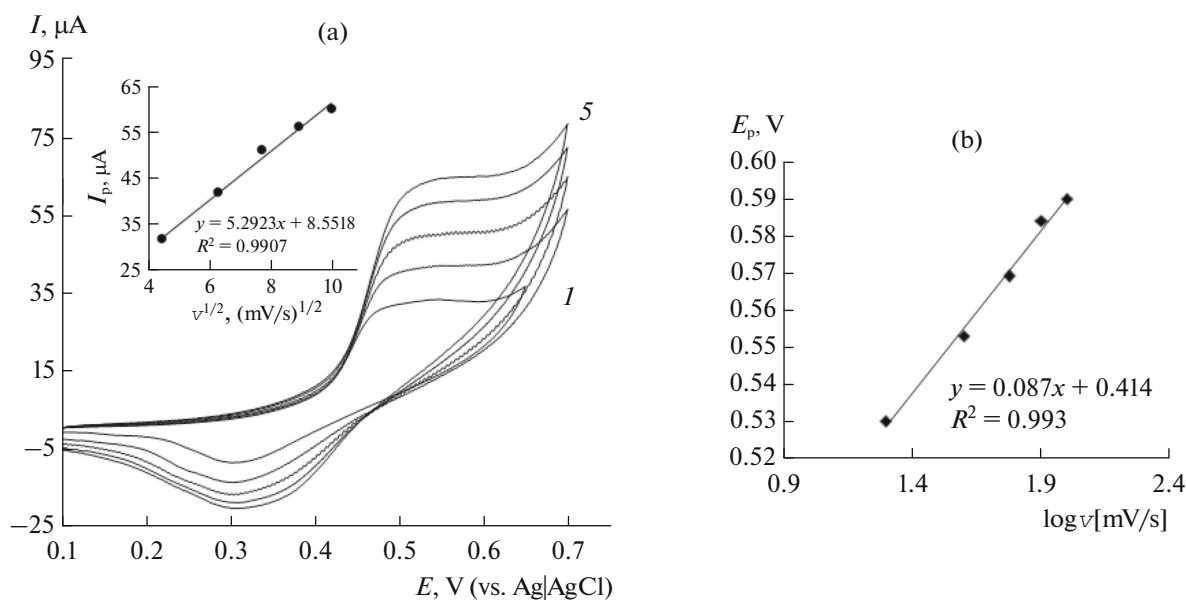


**Fig. 4.** (a)—Cyclic voltammograms of the Ni-NP/MCPE in 0.1 M NaOH solution containing 0.4 mM cabergoline at the scan rates, from 1 to 5: 20, 40, 60, 80, and 100 mV/s. Inset: variation of  $I_{pa}$  vs.  $v^{1/2}$ . (b)—Dependence of the peak potential,  $E_p$ , on  $\log v$  for the oxidation of cabergoline at Ni-NP/MCPE.

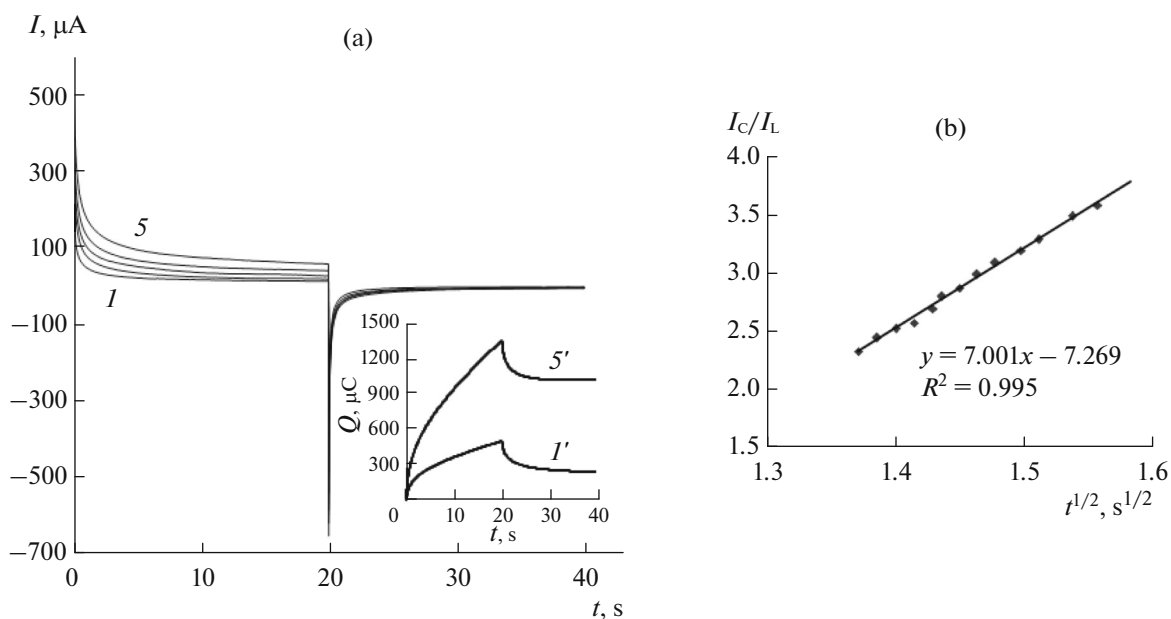


**Fig. 5.** (a)—Chronoamperograms obtained at the Ni-NP/MCPE in the absence ( $I$ ) and presence of 0.2 (2), 0.8 (3), 1.4 (4) and 2.7 (5) mM of cabergoline in 0.1 M NaOH solution, first and second potential steps were 0.55 and 0.30 V (inset). Dependence of  $Q$  ( $\mu\text{C}$ ) vs.  $t$ , ( $I'$ ) and ( $5'$ ), respectively, are derived from the data of chronoamperograms ( $I$ ) and ( $5$ ). (b)—Dependence of  $I_C/I_L$  on  $t^{1/2}$  derived from the data of chronoamperograms of ( $I$ ) and ( $5$ ).

increases, which confirms EC' mechanism. Inset of Fig. 4a shows that the oxidation current for CAB increased linearly with the square root of the scan rate, suggesting that the reaction is mass-transfer controlled. In order to obtain information on the rate-determining step, the Tafel slope,  $b$ , was determined using equation (4), valid for irreversible diffusion controlled process [33]:

$$E_p = (b/2)\log v + \text{constant}. \quad (4)$$

On the basis of the above equation, the slope of  $E_p$  vs.  $\log v$  plot is  $b/2$ , where  $b$  indicates the Tafel slope which was found to be 0.087 V for CAB in this work (Fig. 4b), so,  $b$  is 0.174 V. This slope indicates that a one-electron transfer process is the rate-limiting step, assuming a transfer coefficient of  $\alpha = 0.34$  for CAB.

**Chronoamperometric studies.** Chronoamperometry, as well as other electrochemical methods, was employed for the investigation of electrode processes at chemically modified electrode. Figure 5a shows chronoamperometric measurements of CAB at the Ni-NP/MCPE. These current–time profiles were obtained by setting the working electrode at first potential step of 650 mV and second potential step of 300 mV for various concentrations of CAB. These potential steps were selected according to cyclic voltammogram of the electrode (in chronoamperometric method anodic and cathodic potential steps usually are slightly more positive and less positive than anodic and cathodic peak potentials of cyclic voltammogram, respectively). The forward and backward potential step chronoamperometry of the modified electrode in

the blank solution showed an almost symmetrical chronoamperogram with nearly equal charges consumed for the oxidation and reduction of surface-confined Ni(II)/Ni(III) sites. However, in the presence of CAB, the charge value associated with the forward chronoamperometry,  $Q$ , is greater than that observed for the backward chronoamperometry (inset of Fig. 5). The rate constant for the chemical reaction between CAB and redox sites of Ni-NP/MCPE can be evaluated by the chronoamperometry according to the method described in the literature [34]:

$$I_C/I_L = \gamma^{1/2}[\pi^{1/2}\text{erf}(\gamma^{1/2}) + \exp(-\gamma)/\gamma^{1/2}], \quad (5)$$

where  $I_C$  is the catalytic current of the Ni-NP/MCPE in the presence of CAB,  $I_L$  is the limiting current in the absence of CAB and  $\gamma = kc_0t$  ( $c_0$  is the bulk concentration of CAB) is the argument of the error function. This equation can be used to define the limiting regions of behavior for all EC' mechanism. For small values of  $\gamma$  (e.g.,  $\gamma < 0.05$ ),  $\text{erf}(\gamma^{1/2}) \approx 2\gamma^{1/2}/\pi^{1/2}$ , and  $I_C/I_L \approx 1$  (diffusion pure region); here the catalytic reaction has no effect. For  $\gamma > 1.5$ ,  $\text{erf}(\gamma^{1/2}) \rightarrow 1$ ,  $\exp(-\gamma)/\gamma^{1/2} \rightarrow 0$ , and the equation can be reduced to:

$$I_C/I_L = \gamma^{1/2}\pi^{1/2} = \pi^{1/2}(kc_0t)^{1/2}. \quad (6)$$

This defines the kinetic pure region (KP), where  $I_C/I_L > 2.17$ . In this region the chronoamperometric response can be employed to determine  $\gamma$  (or  $kc_0t$ ). Where  $k$ ,  $c_0$  and  $t$  are the catalytic rate constant ( $\text{cm}^3/(\text{mol s})$ ), CAB concentration (mM) and time elapsed (s), respectively. From the slope of the  $I_C/I_L$

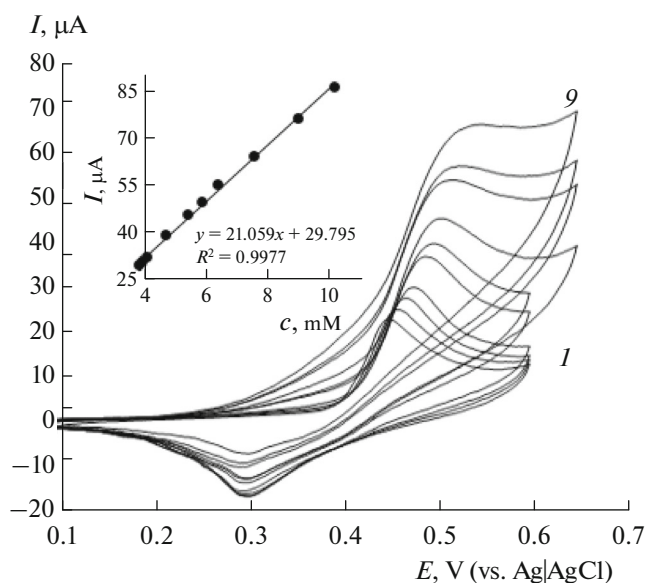


**Fig. 6.** Current–potential curves for oxidation of cabergoline at the Ni-NP/MCPE in 0.1 M NaOH solution with different concentrations of cabergoline: 0 (I), 0.005 (2), 0.05 (3), 0.5 (4), 0.8 (5), 0.1 (6), 1.5 (7), 2 (8) and 2.7 (9) mM. Inset: plot of  $I_p$  versus  $c$ .

vs.  $t^{1/2}$  plot we can simply calculate the value of  $k$  for a given concentration of substrate. Figure 5b shows one such plot, constructed from the chronoamperogram of the Ni-NP/MCPE with and without 2.7 mM CAB. The mean value for ( $k$ ) is  $5.78 \times 10^6 \text{ cm}^3/(\text{mol s})$ .

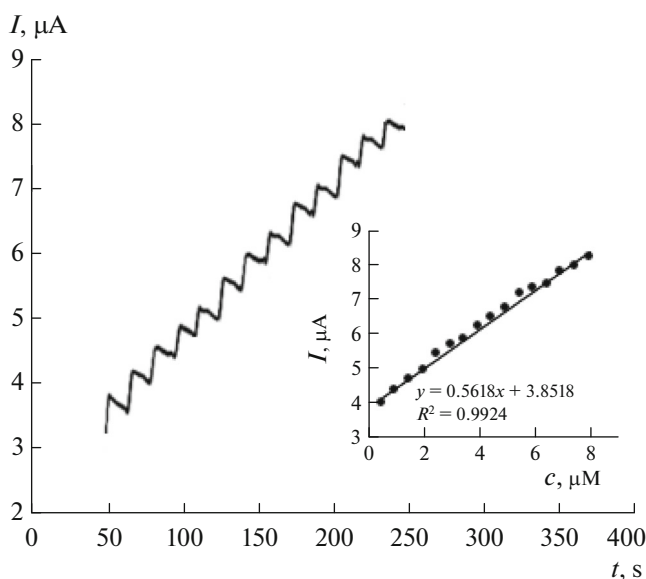


**Fig. 7.** Typical amperograms showing the current response for successive added volumes of 5  $\mu\text{M}$  solution of cabergoline in 0.1 M NaOH solution. Inset: variation of amperometric current vs. cabergoline concentration.

**Electrocatalytic determination of cabergoline.** Figure 6 shows the cyclic voltammograms of the Ni-NP/MCPE in the presence of different concentration of CAB. As can be seen, Ni-NP/MCPE exhibits a well-defined catalytic oxidation current increasing linearly with an increase in CAB concentration. Calibration plots for the determination of CAB show linear dependence of the anodic peak current on CAB concentration (inset of Fig. 6) in the range of 0.005 to 2.7 mM and a correlation coefficient of 0.998. The detection limit, taken as the concentration that gave a signal equal to three times the standard deviation of the blank, calculated from the calibration graph, was 0.002 mM.

Since the cyclic voltammetry is not sensitive for low concentrations of CAB, constant potential amperometry under hydrodynamic conditions was used to detect lower concentrations of CAB. Figure 7 shows a typical hydrodynamic amperometric response obtained by adding CAB to a continuously stirred 0.1 M NaOH solution, which shows an increase in current for successive increments of 5  $\mu\text{M}$  CAB. The inset of Fig. 7 illustrates the corresponding plot showing a linear relationship between peak current and CAB concentrations in the range of  $5 \times 10^{-7}$ – $8 \times 10^{-6}$  M. The detection limit is  $1.5 \times 10^{-7}$  M.

To illustrate the modified electrode application in practical analysis, we used it to detect CAB in human plasma and drug tablet samples. All samples were diluted with 0.1 M NaOH solution and a known amount of CAB was spiked to plasma solution. Standard addition method was used to analyze the prepared samples. The quantity of experimentally determined CAB was compared to that of reported and spiked values in tablet and plasma samples. The results are summarized in table.

\*\*\*

A carbon paste electrode modified with Ni nanoparticles was examined for electrooxidation of CAB in alkaline medium using cyclic voltammetry and chronoamperometry techniques. The kinetic parameters, such as charge-transfer coefficient and catalytic reaction rate constant, were determined. The value of the rate constant ( $k$ ) obtained from the chronoamperometric method indicated that the modified electrode can overcome the kinetic limitations for CAB oxidation by a catalytic process and can decrease the overpotential for the oxidation reaction. According to the experimental results, the catalytic oxidation current of CAB at this electrode can be used to determine this drug in aqueous solution, so that an acceptable linear dynamic range and detection limit can be obtained. An amperometric method was proposed for the determination of CAB with good sensitivity and selectivity in biological media and pharmaceutical formulations.

Results of determination of cabergoline using Ni-NP/MCPE

Sample	Labeled	Added	Found	Recovery, %	RSD, % (n = 3)
Plasma	—	6 $\mu$ M	5.9 $\mu$ M	98.3	1.2
Tablet	1 mg	—	1.05 mg	105	2.5

#### ACKNOWLEDGMENTS

We would like to thank the Islamic Azad University, Ayatollah Amoli Branch for generous financial support of the research project.

#### REFERENCES

1. Cabergoline. <http://en.wikipedia.org/wiki/Cabergoline>. Cited April 14, 2015.
2. Onal, A., Sagirli, O., and Sensoy, D., *Chromatographia*, 2007, vol. 65, nos. 9–10, p. 561.
3. Allievi, C. and Dostert, P., *Rapid, Commun. Mass Spectrom.*, 1998, vol. 12, no. 1, p. 9.
4. Kimball, B.A., DeLiberto, T.J., and Johnston, J., *Anal. Chem.*, 2001, vol. 73, no. 20, p. 4972.
5. Schapira, A.H.V., *J. Neurol., Neurosurg. Psychiatry*, 2005, vol. 76, no. 11, p. 1472.
6. Karlsen, K.H., Tandberg, E., Årslund, D., and Larsen, J.P., *J. Neurol., Neurosurg. Psychiatry*, 2000, vol. 69, p. 584.
7. Chiueh, C.C., Krishna, G., Tulsi, P., Obata, T., Lang, K., and Huang, S.J., *Free Radical Biol. Med.*, 1992, vol. 13, p. 581.
8. Mena, M.A., Casarejos, M.J., Carazo, A., Paino, C.L., and De, J.G., *J. Neural Transm.*, 1997, vol. 104, p. 317.
9. Asanuma, M., Miyazaki, I., and Ogawa, N., *Neurotoxic. Res.*, 2003, vol. 5, p. 165.
10. Nigovic, B. and Simunic, B., *J. Pharm. Biomed. Anal.*, 2003, vol. 31, p. 169.
11. Uslu, B. and Ozkan, S.A., *Electrochim. Acta*, 2004, vol. 49, p. 4321.
12. Parvin, M.H., *Electrochem. Commun.*, 2011, vol. 13, p. 366.
13. Svancara, I., Vytras, K., Kalcher, K., Walcarius, A., and Wang, J., *Electroanalysis*, 2009, vol. 21, p. 7.
14. Mahmoud, K.A., Hrapovic, S., and Luong, J.H., *ACS Nano*, 2008, vol. 2, p. 1051.
15. Streeter, I., Baron, R., and Compton, R.G., *J. Phys. Chem. C*, 2007, vol. 111, p. 1708.
16. Zhang, Y., Suryanarayanan, V., Nakazawa, I., Yoshihara, S., and Shirakashi, T., *Electrochim. Acta*, 2004, vol. 49, p. 5235.
17. Hao, N., Li, H., Zhang, L., Zhao, X., Xu, D., and Chen, H.Y., *J. Electroanal. Chem.*, 2011, vol. 656, p. 50.
18. Penner, R.M. and Martin, C.R., *Anal. Chem.*, 1987, vol. 59, p. 2625.
19. Cassidy, J., Ghoroghchian, J., Sarfarazi, F., Smith, J.J., and Pons, S., *Electrochim. Acta*, 1986, vol. 31, p. 629.
20. Meyer, H., Drewer, H., Gruendig, B., Cammann, K., Kakerow, R., Manoli, Y., and Rospert, M., *Anal. Chem.*, 1995, vol. 67, p. 1164.
21. Huang, J., Liu, Y., Hou, H., and You, T., *Biosens. Bioelectron.*, 2008, vol. 24, p. 632.
22. An, K., Lee, N., Park, J., Kim, S.C., Hwang, Y., Park, J.G., and Hyeon, T., *J. Am. Chem. Soc.*, 2006, vol. 128, p. 9753.
23. Hu, J., Wen, Z., Wang, Q., Yao, X., Zhang, Q., Zhou, J., and Li, J., *J. Phys. Chem. B*, 2006, vol. 110, p. 24305.
24. Li, W.Y., Xu, L.N., and Chen, J., *Adv. Funct. Mater.*, 2005, vol. 15, p. 851.
25. Ojani, R., Raoof, J.B., and Zamani, S., *Electroanalysis*, 2009, vol. 21, p. 2634.
26. Ojani, R., Raoof, J.B., and Zamani, S., *Bioelectrochemistry*, 2012, vol. 85, p. 44.
27. Ojani, R., Raoof, J.B., and Zamani, S., *Talanta*, 2010, vol. 81, p. 1522.
28. Fathi, S., *Russ. J. Electrochem.*, 2014, vol. 50, p. 468.
29. Roselina, N., Azizan, A., and Lockman, Z., *Sains Malays.*, 2012, vol. 41, p. 1037.
30. Pham, M.T., Maitz, M.F., Richter, E., Reuther, H., Prokert, F., and Mucklich, A., *J. Electroanal. Chem.*, 2004, vol. 572, p. 185.
31. Mirceski, V. and Gulaboski, R., *Electroanalysis*, 2001, vol. 13, p. 1326.
32. Mirceski, V. and Gulaboski, R., *Electroanalysis*, 2003, vol. 7, p. 157.
33. Priente, F., Lorenzo, E., Tobalina, F., and Abruna, H.D., *Anal. Chem.*, 1995, vol. 67, p. 3936.
34. Bard, A.J. and Faulkner, L.R., *Electrochemical Methods*, New York: Wiley, 2001.